



N_2O -based climatology of the Brewer-Dobson Circulation in WACCM, a chemical reanalysis and a CTM driven by four dynamical reanalyses

Daniele Minganti⁽¹⁾, Simon Chabrillat⁽¹⁾, Yves Christophe⁽¹⁾, Quentin Errera⁽¹⁾, Marta Abalos⁽²⁾, Maxime Prignon⁽³⁾, Douglas Kinnison⁽⁴⁾, Emmanuel Mahieu⁽³⁾

⁽¹⁾Belgian Institute of Space Aeronomy, BIRA-IASB, Brussels, 1180 Belgium. ⁽²⁾Universidad Complutense de Madrid, Madrid, Spain. ⁽³⁾Institute of Astrophysics and Geophysics, University of Liège, 4000 Liège, Belgium. ⁽⁴⁾National Center for Atmospheric Research, Boulder, CO, USA

EGU2020: Sharing Geoscience Online

EGU2020-7432

AS3.5 Dynamics and chemistry of the upper troposphere and stratosphere

05/05/2020 14:00-15:45

[*Minganti et al., ACPD, \(2020\)*](#)

Outline

[Introduction](#)

[Methods](#)

[Seasonal means](#)

[Mean annual cycle](#)

[Variability](#)

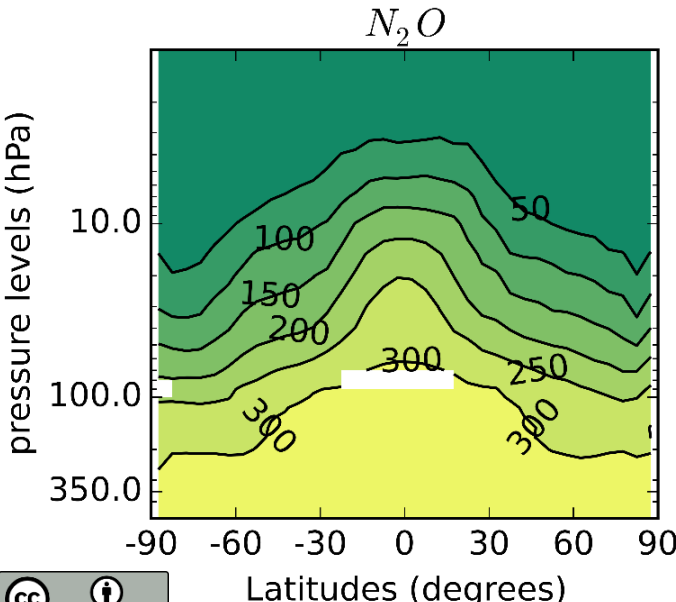
[Conclusions](#)

[References](#)

Introduction

Brewer-Dobson Circulation (BDC): stratospheric circulation that consists in a slow upwelling in the Tropics from the troposphere into the stratosphere, followed by poleward transport and downwelling at higher latitudes in winter.

For tracer-transport purposes the BDC is often divided into an advective component, the residual mean meridional circulation (white arrows in Fig. 1), and a quasi-horizontal two-way mixing which causes net transport of tracers (orange arrows in Fig. 1).



N_2O (nitrous oxide): long-lived tracer to study the BDC (lifetime ~120 years). Its distribution is dominated by dynamics (Fig. 2).

Fig. 2. Annual N_2O mixing ratio [ppbv] climatology, from February 2004 until February 2013 using ACE-FTS v3.5 data products (Koo et al., JQS&RT, 2017).

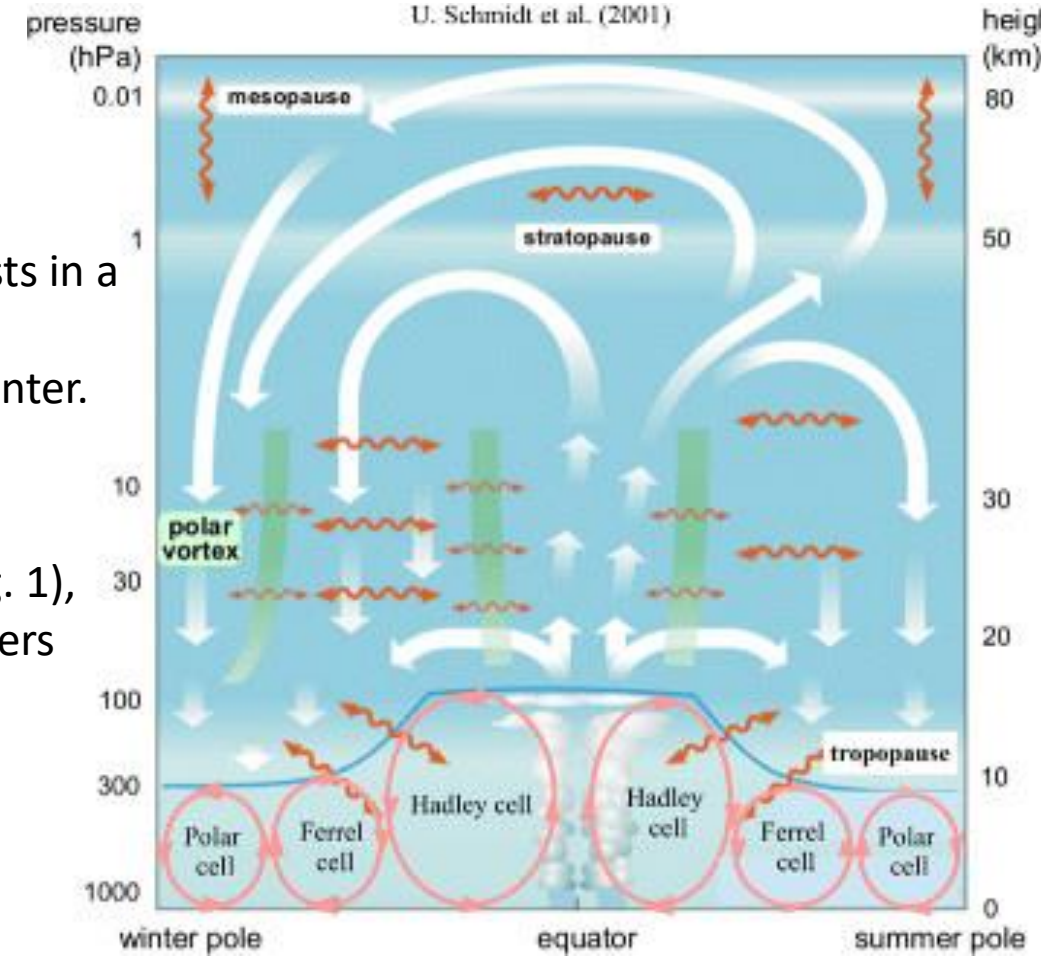


Fig. 1. Schematic of the BDC as the combined effect of residual circulation and mixing. The thick white arrows depict the residual circulation whereas the wavy orange arrows indicate two-way mixing processes. The thick green lines represent stratospheric transport and mixing barriers. From Bonisch et al., ACP, (2011).

Methods

Considered period: January 2005 to December 2014 (10 years).

WACCM (Whole Atmosphere Community Climate Model, *Garcia et al., JAS, 2017*).

- 3 realizations of the CCM4 version with modified gravity waves parameterization (*Garcia et al., JAS, 2017*).
- 1 realization of WACCM4 (*Marsh et al., JC, 2013*)
- longitude-latitude grid of $2.5^\circ \times 1.9^\circ$ and 66 vertical levels from the surface to about 140 km altitude.

BASCOE CTM (Belgian Assimilation System for Chemical ObsErvations, *Chabrillat et al., ACP, 2018*)

- Chemistry-Transport Model: kinematic transport (FFSL advection scheme), explicit solver for stratospheric chemistry (*Prignon et al., ACP, 2019*).
- Latitude-longitude grid ($2.5^\circ \times 2^\circ$). Keep the native vertical grids of the dynamical reanalyses: ERAI and JRA55 have 60 levels up to 0.1 hPa while MERRA and MERRA2 have 72 levels up to 0.01 hPa.
- Dynamical Reanalyses: the European Centre for Medium-Range Weather Forecasts Interim Reanalysis (ERA-Interim, hereafter ERAI; *Dee et al., QJRMS, 2011*), the Japanese 55-year Reanalysis (JRA55; *Kobayashi et al., JMS, 2015*), the Modern-Era Retrospective analysis for Research and Applications (MERRA; *Rienecker et al., JC, 2011*) and its version 2 (MERRA2; *Gelaro et al., JC, 2017*).

BRAM2 (BASCOE Reanalysis of Aura MLS version 2, *Errera et al., ACP, 2019*):

- Chemical reanalysis: assimilates the N₂O product of Aura MLS.
- Period of assimilation: August 2004-August 2019.
- BRAM2 is driven by ERA-Interim, with a horizontal resolution of $3.75^\circ \times 2.5^\circ$ and 37 hybrid pressure levels.



Methods

Transformed Eulerian Mean (TEM, Andrews *et al.* 1987) allows to separate the local rate of change of a tracer (N_2O) in terms due to transport and chemistry.

N_2O continuity equation:

$$\bar{\chi}_t = -\bar{v}^* \bar{\chi}_y - \bar{w}^* \bar{\chi}_z + e^{z/H} \nabla \cdot \mathbf{M} + \bar{S},$$

\mathbf{M} vector components:

$$M^{(y)} \equiv -e^{-z/H} (\bar{v}' \chi' - \bar{v}' \theta' \bar{\chi}_z / \bar{\theta}_z),$$

$$M^{(z)} \equiv -e^{-z/H} (\bar{w}' \chi' + \bar{v}' \theta' \bar{\chi}_y / \bar{\theta}_z),$$

We define:

$$A_y = -\bar{v}^* \bar{\chi}_y,$$

$$M_y = e^{z/H} \cos\phi^{-1} (M^{(y)} \cos\phi)_y,$$

$$A_z = -\bar{w}^* \bar{\chi}_z,$$

$$M_z = e^{z/H} (M^{(z)})_z,$$

$$\chi = N_2O \quad H = 7\text{km} \quad p_s = 10^5 \text{Pa}$$

$$z \equiv -H \log_e(p/p_s) \quad \bar{S} = \bar{P} - \bar{L}$$

Vertical and meridional residual velocity components:

$$\bar{v}^* \equiv \bar{v} - e^{z/H} (e^{-z/H} \bar{v}' \theta' / \bar{\theta}_z)_z,$$

$$\bar{w}^* \equiv \bar{w} + (\cos\phi)^{-1} (\cos\phi \bar{v}' \theta' / \bar{\theta}_z)_\phi.$$

N_2O continuity equation:

$$\bar{\chi}_t = A_y + M_y + A_z + M_z + (\bar{P} - \bar{L}) + \bar{\epsilon},$$

Vertical advection term [ppbv/day]

Horizontal mixing term [ppbv/day]

- v , w and θ are respectively the Eulerian zonal-mean meridional and vertical velocities and potential temperature.
- ϕ is the latitude, and S is the net rate of change due to chemistry, where P and L are respectively the chemical production and loss rates.
- Overbar quantities represent zonal mean fields, primed quantities the departures from the zonal mean, and subscripts denote derivatives.
- Meridional derivatives are evaluated in spherical coordinates and vertical derivatives with respect to log-pressure altitude z .

TEM budget

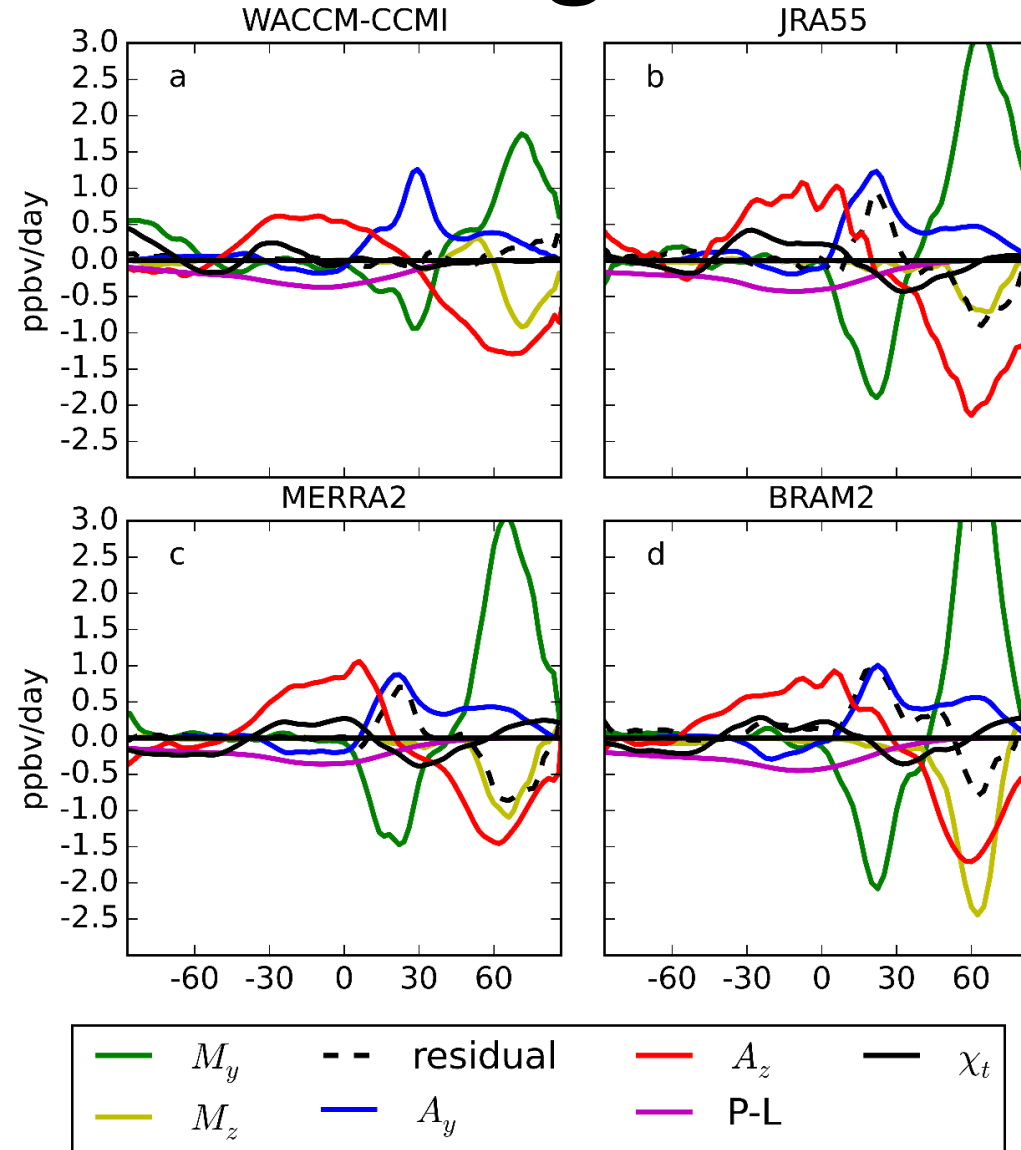


Fig. 3. Latitudinal profiles of the N_2O TEM budget terms [ppbv/day] at 15 hPa averaged in DJF (2005-2014). Top row (left to right): WACCM-CCMI (a), JRA55 (b); bottom row (left to right) MERRA2 (c) and BRAM2 (d).

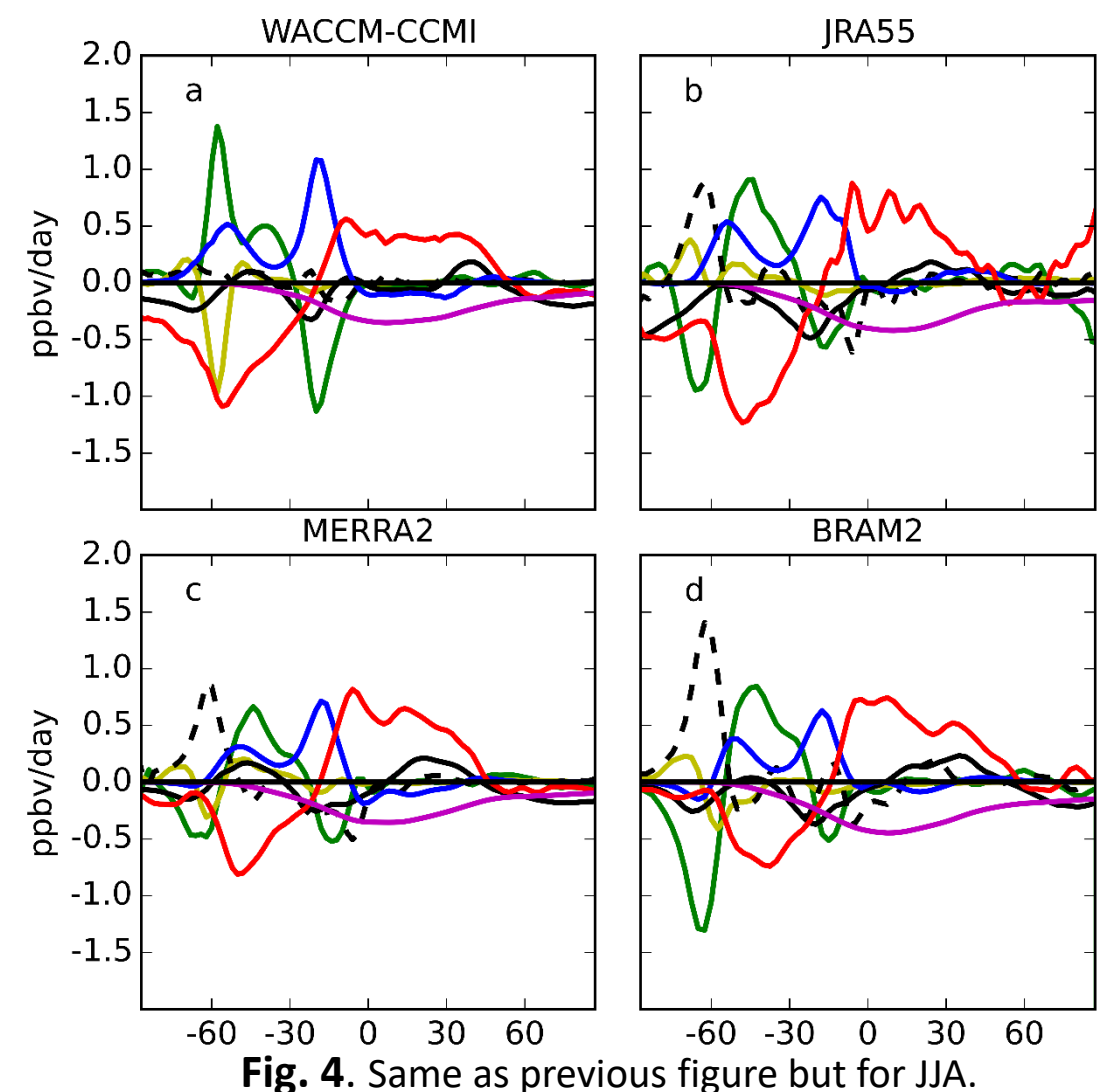


Fig. 4. Same as previous figure but for JJA.

Compensation of the TEM N_2O budget terms to recover the N_2O time derivative (Figs. 1 and 2).

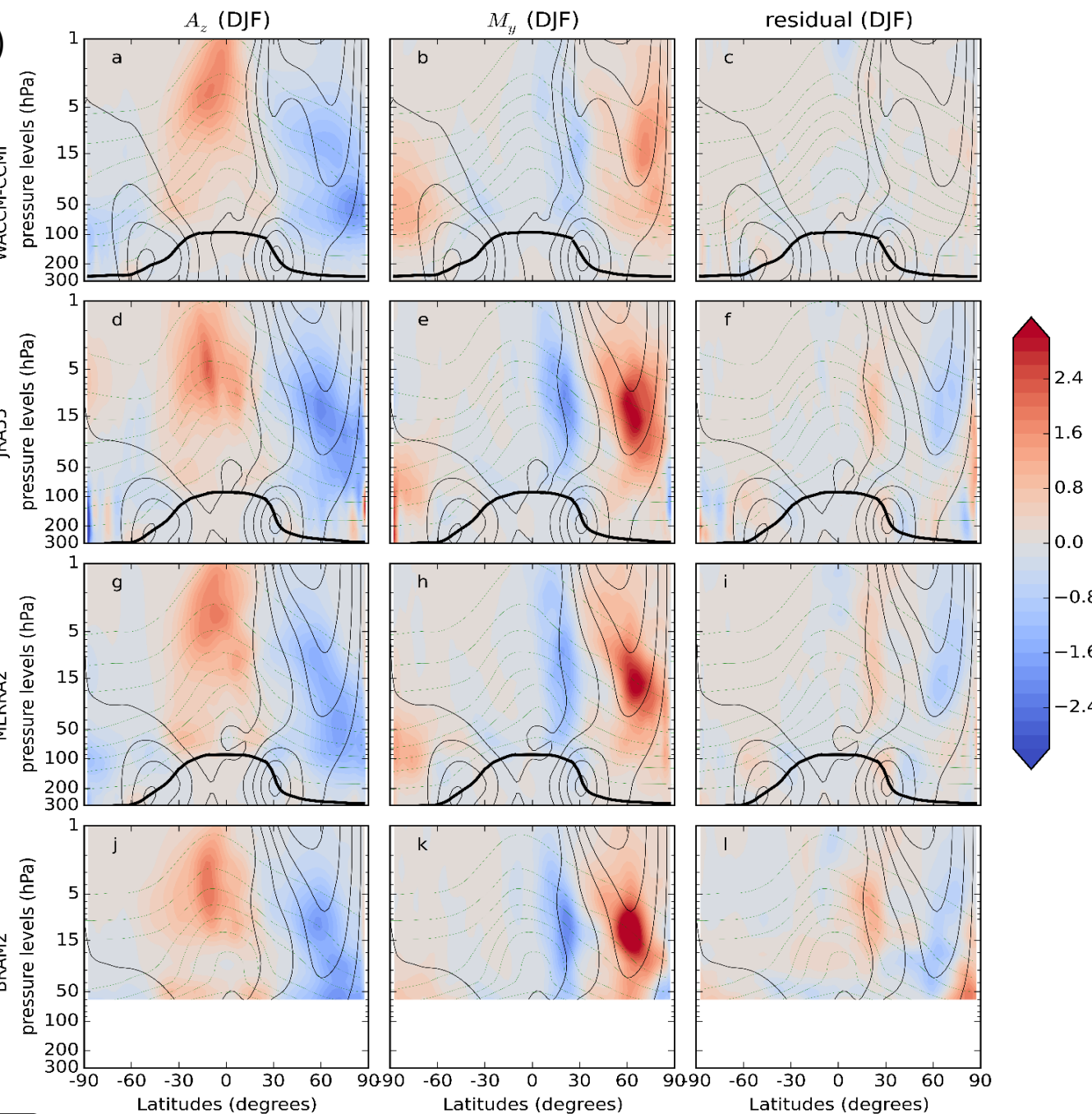
Red: N_2O increase ($dN_2O/dt > 0$). Blue: N_2O decrease ($dN_2O/dt < 0$)

Seasonal mean

Vertical advection term A_z : the tropical upwelling increases the N_2O abundances in the mid-high stratosphere. The downwelling decreases it in the high latitudes in the middle and low stratosphere (Figs. 5 and 6).

Horizontal mixing term M_y : increases N_2O abundances in the surf zone (Figs. 5 and 6).

Fig. 5. Climatological (2005-2014) latitude-pressure cross sections of three N_2O TEM budget terms averaged in DJF [ppbv/day]: horizontal mixing term (left column), vertical residual advection term (central column) and residual term (right column). The datasets are, from top to bottom: WACCM-CCMI, JRA55, MERRA2, and BRAM2. The residual term for WACCM-CCMI is from a single realization of the model. The thin black lines show the zonal mean zonal wind (from 0 to 40 m/s every 10 m/s), the black thick line represents the dynamical tropopause for the considered season and the green thin lines show the climatological mixing ratio of N_2O (from 20 to 300 ppbv with 40 ppbv spacing).



Red: N_2O increase ($dN_2O/dt > 0$). Blue: N_2O decrease ($dN_2O/dt < 0$)

Seasonal mean

Horizontal mixing term M_y : tends to reduce the meridional gradients of N_2O generated by the residual advection.

During winter it presents large hemispheric differences (Figs. 5 and 6).

Horizontal mixing term M_y : transport barriers are identified in regions where it has a strong meridional gradient (red/blue transition regions, Figs. 5 and 6).

Above the Antarctic the negative M_y is balanced by the residual in the reanalyses (Fig. 6).

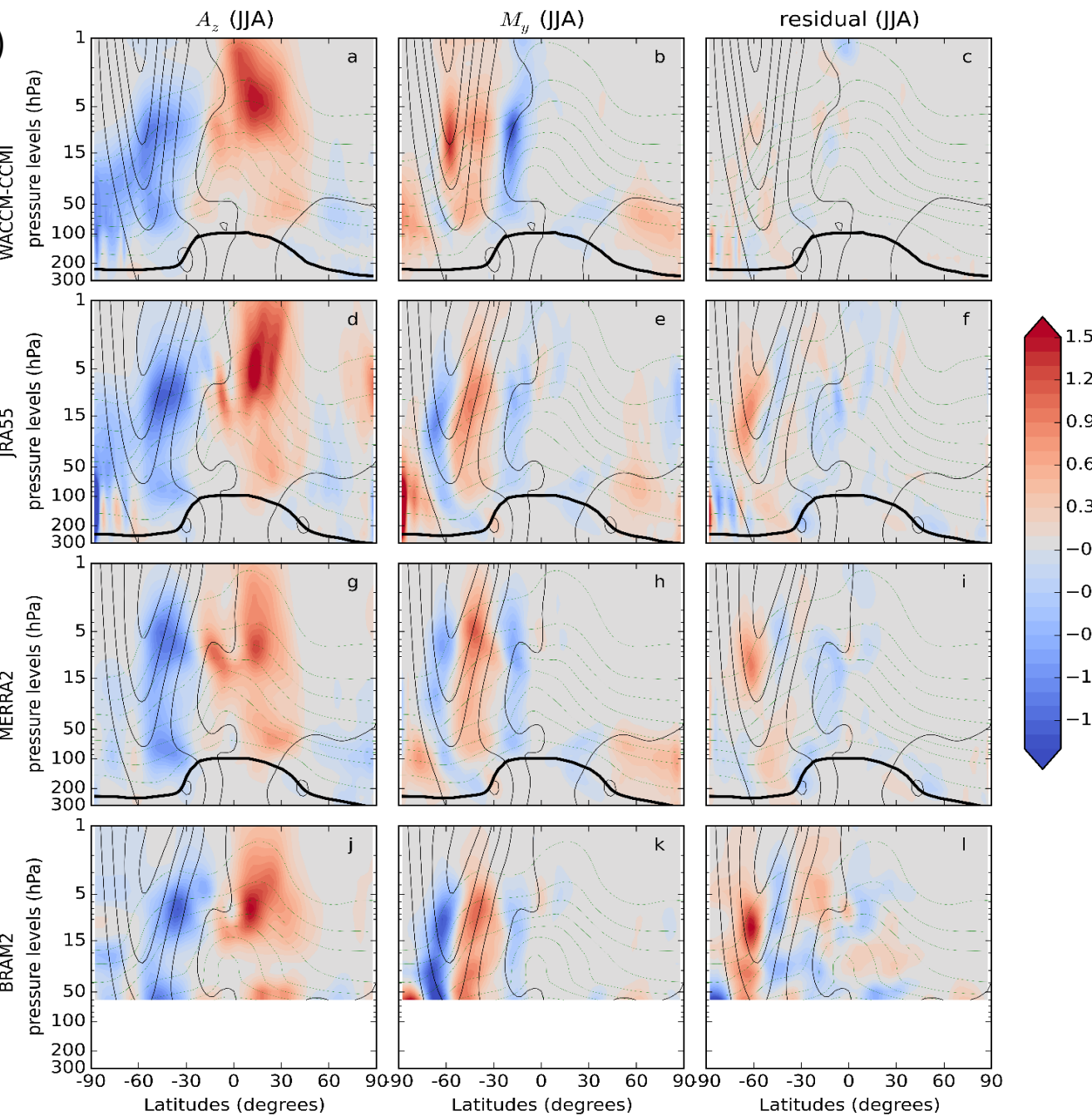


Fig. 6. Same as previous figure but for JJA and with a different color scale. The thin black contours show the zonal mean zonal wind (from 0 to 100 m/s every 20 m/s).

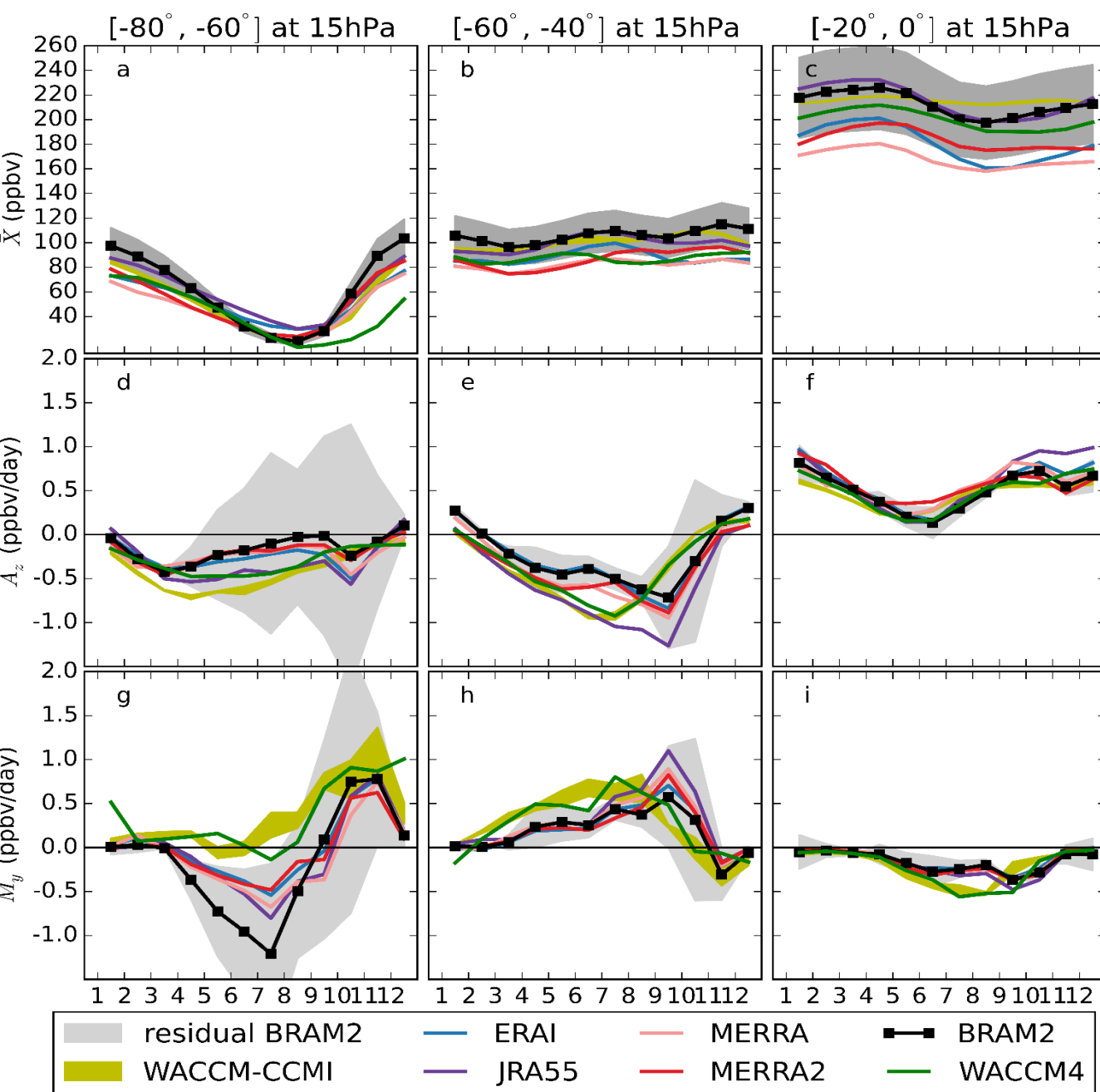
Mean annual cycle

N_2O mixing ratio: large differences in the Tropics.

Vertical advection term A_z : general agreement in the Tropics.

Horizontal mixing term M_y : large differences in the Antarctic region and large residual.

Fig. 7. Monthly mean annual cycles at 15 hPa in the SH. First row: N_2O volume mixing ratio [ppbv], second row: horizontal mixing term [ppbv/day]; third row: vertical residual advection term [ppbv/day]. Left column: polar region (60° - 80° S), middle column: midlatitudes (40° - 60° S), right column: Tropics (0° - 20° S). The olive envelope shows the 3 realizations of the WACCM-CCMI simulation. The dark grey shading (top row) shows 15% uncertainty around BRAM2. The light grey shading (middle and bottom rows) shows BRAM2 plus and minus the residual term.



Mean annual cycle

N_2O abundances: large disagreement in the Tropics.

Vertical advection term A_z : good agreement among the datasets.

Horizontal mixing term M_y : smaller in absolute value in WACCM than the reanalyses.

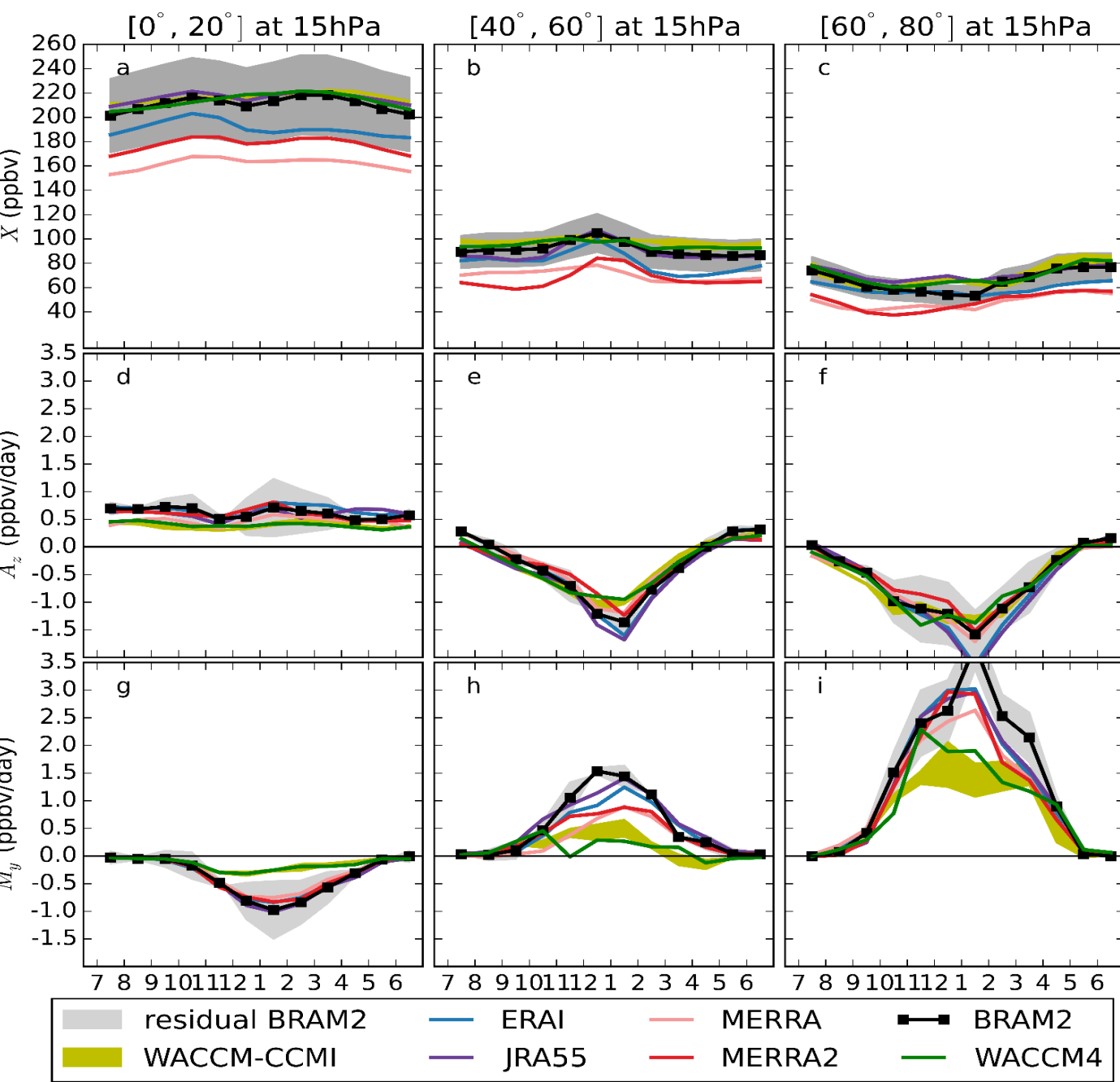


Fig. 8. Same as previous figure but showing the NH and with different vertical limits.

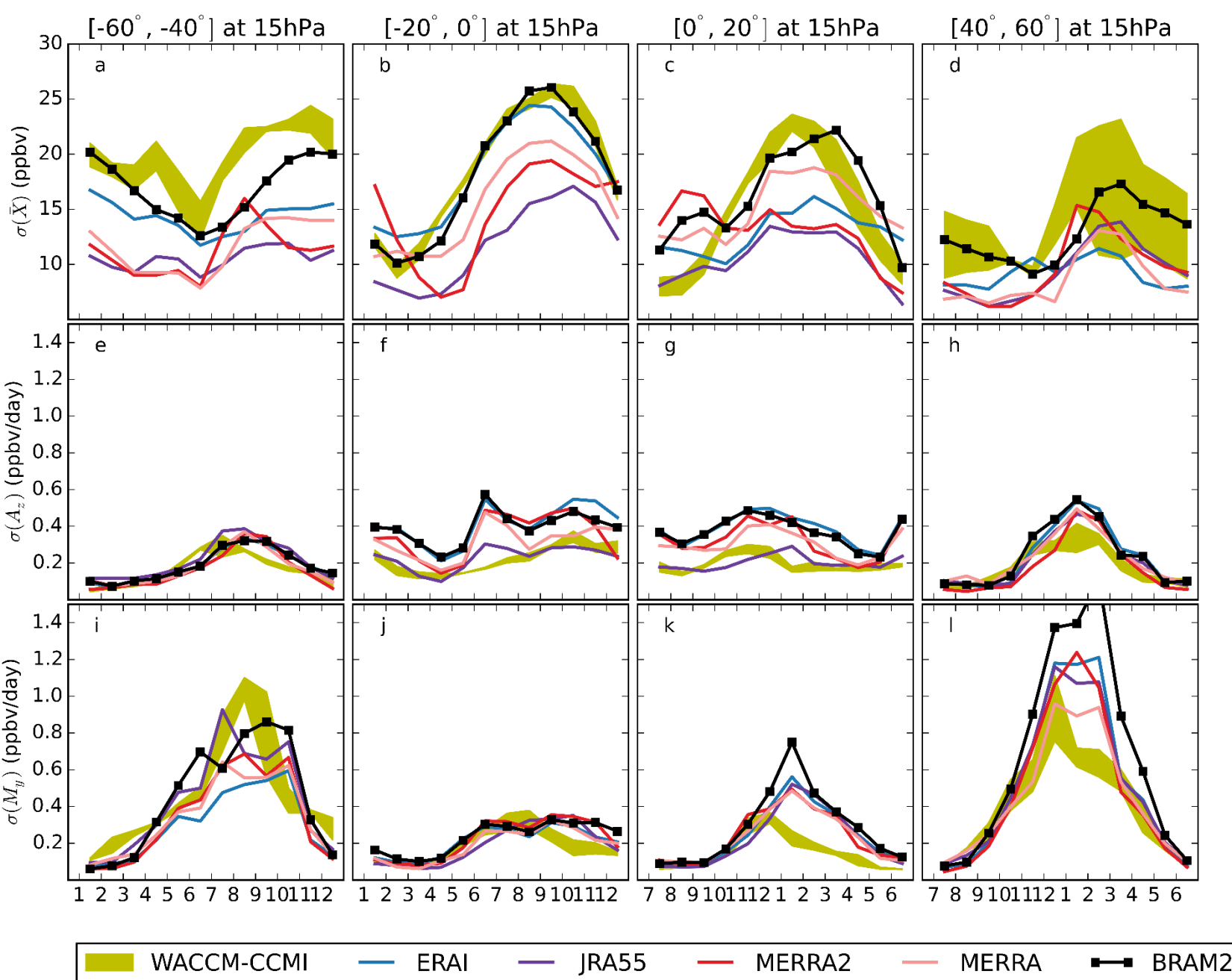
Variability

N_2O mixing ratio: WACCM agrees with BRAM2. The dynamical reanalyses deliver smaller variability.

Vertical advection term A_z : marked differences in the Tropics.

Horizontal mixing term M_y : large variability in the middle latitudes.

Fig. 9. Monthly standard deviation over 2005-2014 at 15 hPa. First row: N_2O volume mixing ratio [ppb], second row: horizontal mixing term [ppbv/day]; third row: vertical residual advection term [ppbv/day]. From left to right: southern mid-latitudes (40° - 60° S), southern tropics (0° - 20° S), northern tropics (0° - 20° N), northern mid-latitudes (40° - 60° N). The yellow envelope shows the 3 realizations of the WACCM-CCMI simulation.



Variability

N_2O mixing ratio, horizontal mixing term M_y and vertical advection term A_z : larger variability in spring over the Antarctic.

Vertical advection term A_z and horizontal mixing term M_y : larger variability above the Arctic during winter.

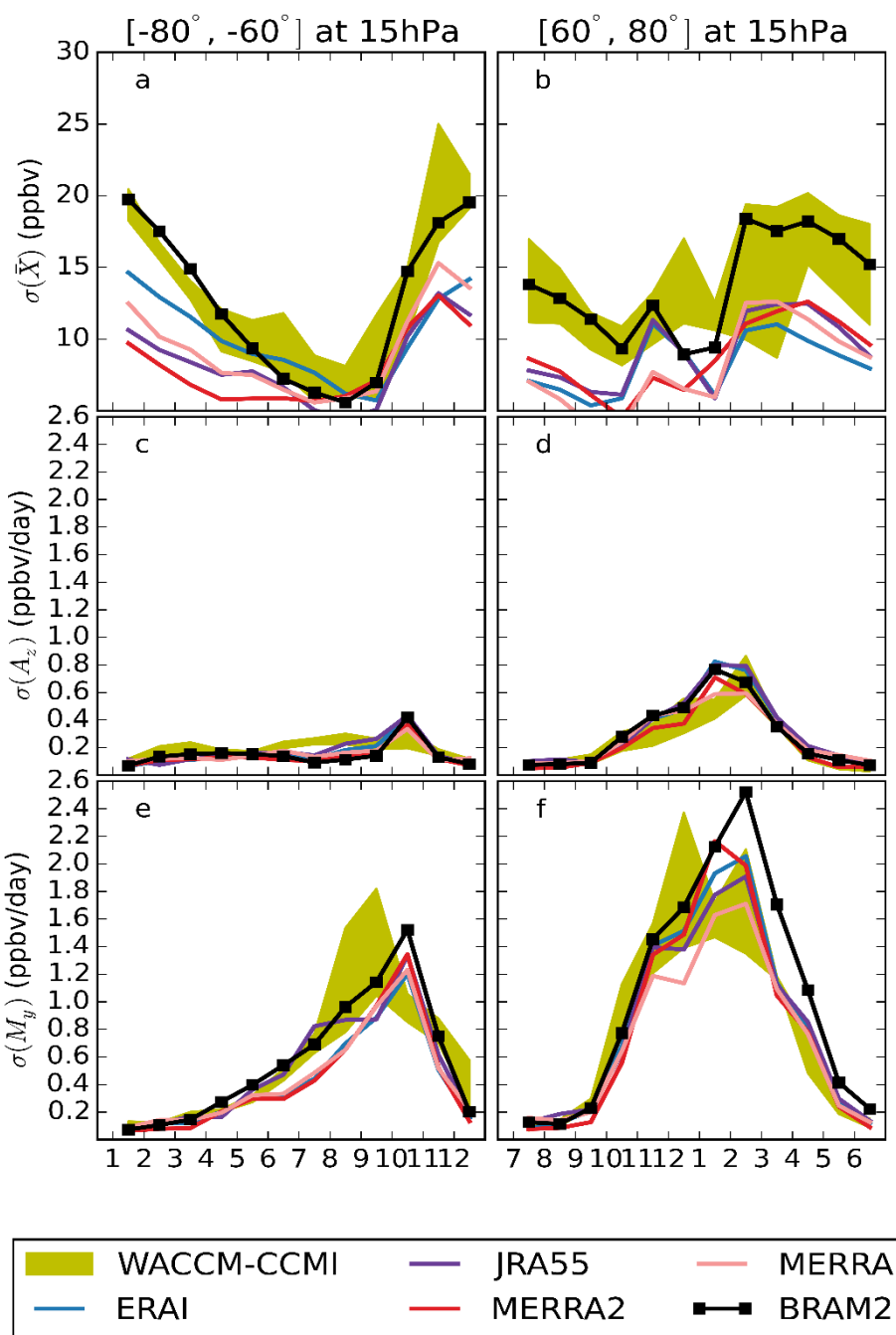


Fig. 10. Same as previous figure but for the polar regions (left column: Antarctic region, 80° - 60° S; right column: arctic region, 60° - 80° N). The vertical scale for the TEM budget terms also differs from the previous figure.

Conclusions

- N_2O mixing ratio in the middle stratosphere (Figs. 7 and 8): agreement in the annual cycle. Large spread of the CTM experiments ($\sim 20\%$) in the Tropics reflecting the differences in mean Age of Air obtained with the same model (*Chabriat et al., ACP, 2018*).
- Vertical advection term A_z : general agreement among the datasets, especially in the NH where WACCM follows closely the reanalyses (Figs. 5 and 8).
- Horizontal mixing term M_y :
 - in the NH WACCM simulates a weaker impact of the horizontal mixing compared to the reanalyses (Fig. 5).
 - In the wintertime southern tropics and middle latitudes it is stronger in WACCM than in the reanalyses (Fig. 7).
 - Striking differences in the wintertime Antarctic (where the polar vortex has a major role, Figs. 6 and 7). The horizontal mixing plays an important role in that region in the reanalyses, but not in WACCM. This large wintertime M_y in the reanalyses is challenged by the large residual term.
- Sensitivity test: additional WACCM run (WACCM4) with different gravity waves in the SH. Small impact on the horizontal mixing term M_y , but significant modifications the vertical advection term A_z and the N_2O mixing ratio in the Antarctic (Figs. 7 and 8).
- Inter-annual variability of M_y : largest in the polar regions (Fig. 10). In the Antarctic is related to the vortex breakup during spring, while in the Arctic to the very variable vortex during winter. Inter-annual variability of A_z : large spread in the mid-stratospheric tropical regions (WACCM-CCMI and JRA55 the smallest, Fig. 9).
- The N_2O TEM budget in the reanalyses suffers from a poor closure in the Antarctic region (i.e. large residual term). Detailed studies of transport in the polar stratosphere are thus needed, e.g. comparing the residual circulations with indirect estimates, and evaluating the effective diffusivity (*Abalos et al., QJRMS, 2016*).
- The next step of this research consists in the analysis of the inter-annual variations of the BDC, including the impact of the QBO and the El-Nino Southern Oscillation. Further extensions of this work would include the addition of new reanalysis products such as ERA5 and an intercomparison of several CCMs.



References

- Abalos, M., Legras, B., and Shuckburgh, E.: Interannual variability in effective diffusivity in the upper troposphere/lower stratosphere from reanalysis data, *Quarterly Journal of the Royal Meteorological Society*, 142, 1847–1861, 2016.
- Andrews, D. G., Leovy, C. B., & Holton, J. R. (1987). Middle atmosphere dynamics. Academic press.
- Bönisch, H., Engel, A., Birner, T., Hoor, P., Tarasick, D. W., & Ray, E. A. (2011). On the structural changes in the Brewer-Dobson circulation after 2000. *Atmospheric Chemistry and Physics*, 11(8), 3937.
- Chabriat, S., Vigouroux, C., Christophe, Y., Engel, A., Errera, Q., Minganti, D., ... & Mahieu, E. (2018). Comparison of mean age of air in five reanalyses using the BASCOE transport model. *Atmospheric Chemistry and Physics*, 18, 14715-14735.
- Dee, D. P., Uppala, S., Simmons, A., Berrisford, P., Poli, P., Kobayashi, S., Andrae, U., Balmaseda, M., Balsamo, G., Bauer, d. P., et al.: The ERA-Interim reanalysis: Configuration and performance of the data assimilation system, *Quarterly Journal of the royal meteorological society*, 137, 553–597, 2011.
- Errera, Q., Chabriat, S., Christophe, Y., Debosscher, J., Hubert, D., Lahoz, W., Santee, M. L., Shiotani, M., Skachko, S., von Clarmann, T., and Walker, K.: Technical note: Reanalysis of Aura MLS chemical observations, *Atmos. Chem. Phys.*, 19, 13647-13679, <https://doi.org/10.5194/acp-19-13647-2019>, 2019.
- Garcia, R. R., Smith, A. K., Kinnison, D. E., Cámará, Á. D. L., & Murphy, D. J. (2017). Modification of the gravity wave parameterization in the Whole Atmosphere Community Climate Model: Motivation and results. *Journal of the Atmospheric Sciences*, 74(1), 275-291.
- Gelaro, R., McCarty, W., Suárez, M. J., Todling, R., Molod, A., Takacs, L., Randles, C. A., Darmenov, A., Bosilovich, M. G., Reichle, R., et al.: The modern-era retrospective analysis for research and applications, version 2 (MERRA-2), *Journal of Climate*, 30, 5419–5454, 2017.
- Kobayashi, S., Ota, Y., Harada, Y., 630 Ebita, A., Moriya, M., Onoda, H., Onogi, K., Kamahori, H., Kobayashi, C., Endo, H., et al.: The JRA-55 reanalysis: General specifications and basic characteristics, *Journal of the Meteorological Society of Japan. Ser. II*, 93, 5–48, 2015.
- Koo, J. H., Walker, K. A., Jones, A., Sheese, P. E., Boone, C. D., Bernath, P. F., & Manney, G. L. (2017). Global climatology based on the ACE-FTS version 3.5 dataset: Addition of mesospheric levels and carbon-containing species in the UTLS. *Journal of Quantitative Spectroscopy and Radiative Transfer*, 186, 52-62.
- Marsh, D. R., Mills, M. J., Kinnison, D. E., Lamarque, J.-F., Calvo, N., and Polvani, L. M.: Climate change from 1850 to 2005 simulated in CESM1 (WACCM), *Journal of climate*, 26, 7372–7391, 2013.
- Minganti, D., Chabriat, S., Christophe, Y., Errera, Q., Abalos, M., Prignon, M., Kinnison, D. E., and Mahieu, E.: Climatological impact of the Brewer–Dobson Circulation on the N₂O budget in WACCM, a chemical reanalysis and a CTM driven by four dynamical reanalyses, *Atmos. Chem. Phys. Discuss.*, <https://doi.org/10.5194/acp-2020-262>, in review, 2020.
- Prignon, M., Chabriat, S., Minganti, D., O'Doherty, S., Servais, C., Stiller, G., Toon, G. C., Vollmer, M. K., and Mahieu, E.: Improved FTIR retrieval strategy for HCFC-22 (CHClF₂), comparisons with in situ and satellite datasets with the support of models, and determination of its long-term trend above Jungfraujoch, *Atmospheric Chemistry and Physics Discussions*, 2019.
- Rienecker, M. M., Suarez, M. J., Gelaro, R., Todling, R., Bacmeister, J., Liu, E., Bosilovich, M. G., Schubert, S. D., Takacs, L., Kim, G.-K., 685 et al.: MERRA: NASA2°019s modern-era retrospective analysis for research and applications, *Journal of climate*, 24, 3624–3648, 2011.

